Spectroscopic study of polycrystalline TiO_2 doped with vanadium

A. I. Kokorin,[a] V. M. Arakelyan,[b] and V. M. Arutyunian[b]*

[a]N. N. Semenov Institute of Chemical Physics, Russian Academy of Sciences,
4 ul. Kosygina, 119991 Moscow, Russian Federation.
Fax: +7 (095) 137 6130. E-mail: kokorin@chph.ras.ru
[b]Yerevan State University,
1 ul. Manukyana, 375049 Yerevan, Republic of Armenia.
Fax: (374 1) 15 1087

The structure of coordination sites (V^{4+} ions) and their spatial distribution in the polycrystalline titanium dioxide (rutile) lattice were studied by ESR. It was found that at low degrees of doping, at $[V^{4+}] < 0.5$ at.%, the vanadium ions are isotropically distributed in the rutile lattice. At $[V^{4+}] > 0.5$ at.% a new microphase with the mixed composition $\{TiO_2—VO_2\}$ is formed. The mixed microphase has a noticeably narrower band gap than the initial TiO_2. Comparison of the photocurrent spectra and the plots of the integral photocurrent *vs.* vanadium content with the structural data obtained using ESR spectroscopy showed that the formation of the $\{TiO_2—VO_2\}$ microphases deteriorates the photoelectrochemical properties of the modified photoelectrodes. Synthetic procedures interfering the formation of such microphases in the doped rutile are discussed.

Key words: rutile, vanadium, semiconductor doping; structure, photosensitivity; photoelectrochemistry, ESR spectroscopy.

Numerous works during recent 25 years have been devoted to studies of titanium dioxide. This is primarily associated with its wide use (in the form of anatase or rutile) as a support in the development of practically important titanium-vanadium catalysts.[1,2] Since TiO_2 is accessible, ecologically safe, and possesses semiconducting properties, it is a promising starting material for the development of efficient photocatalysts for decomposition of highly toxic organic, including organochloric, substances[3—6] and electrodes for photoelectrochemical conversion of solar energy.[7—10]

The main disadvantage of TiO_2 as a photoactive material is the large gap of the forbidden band ($E_g = 3.1$ eV for rutile and ~3.0 eV for anatase) of the semiconductor, which can absorb photons only in the UV region of the solar spectrum with the wavelength $\lambda < 400$ nm. One of the routes for enhancement of the photosensitivity of TiO_2 and improvement of its photochemical properties at $\lambda > 400$ nm is doping with electroactive admixtures, *i.e.*, transition metal ions.[11,12] The doping of monocrystalline (MC) and polycrystalline (PC) TiO_2 in the rutile form considerably changes the electrophysical and photoelectrochemical properties of these materials.[11—15] The spectral sensitivity of the TiO_2 electrodes was extended markedly to the long-wave region using their doping with the V^{4+} and Cr^{3+} ions.[12,14—16]

The influence of dopants on the semiconducting and photoelectrochemical properties of TiO_2 has been studied in detail. However, no sufficient attention was given to analysis of the structure of these systems and, first of all, to the space distribution of dopants in the TiO_2 matrix. The randomness of distribution of acceptor admixtures (V^{4+} ions) in PC rutile or heterogeneity of its matrix has a strong influence on the electrophysical properties. Knowing the spatial organization of the matrix of electrodes, one can recommend pathways for improvement of the technology of their manufacturing. This work is devoted to the elucidation of the specific features of the structure and properties of PC TiO_2 (rutile) doped with the V^{4+} ions using different spectroscopic and electrochemical methods.

Experimental

Powders of TiO_2 and the doping admixture (VO_2) (specially pure grade) were used as the initial material for the preparation of samples. The samples were synthesized by the solid-phase reaction. The initial oxides were taken in a required ratio, thoroughly stirred, and molded to form bricks, which were subjected to thermal treatment for 2 h at 1200 °C in an inert medium (He). Two series of samples were prepared. In the first series (V-1), after the thermal treatment, the matrix contained an uncontrolled amount of oxygen vacancies. To remove the latter, after high-temperature annealing, the samples of the V-2 series were additionally annealed in air for 2 h at 900 °C. Due to the dopant atoms and oxygen vacancies, after doping the samples gained a uniform dark color both on the surface and in the bulk.

Published in Russian in *Izvestiya Akademii Nauk. Seriya Khimicheskaya,* No. 1, pp. 88—92, January, 2003.

Homogeneity of the resulting samples was monitored by X-ray diffraction analysis, which showed that all doped samples up to the vanadium content of 5 at.% retained uniformity and had the structure of the initial rutile.[17]

For photoelectrochemical and optical measurements, the bricks were cut into plates 1.0 mm thick and both sides were thoroughly polished. Then an indium or copper layer was deposited on one of the sides by vacuum sputtering to create an ohmic contact. For ESR studies, a part of the doped sample was ground to a particle size of 30—100 μm.

Electroconductivity of the samples was measured by the standard four-probe method. The spectral plot of the photocurrent was determined as follows. The light from a DKSSh-1000 high-pressure xenon lamp passed through an optical system and a modulator and came to the monochromator inlet in an SF-16 spectrophotometer. At the outlet the light was focused on a photoanode, which was placed in a photoelectrolysis cell. The photoresponse was given to the first inlet of a synchronous detector, and the signal from the load resistance of the inversely biased photodiode came to the second inlet. Then the signal got on a KSP-4 detector.

ESR spectra were recorded on a Varian E-3 radiospectrometer at 77 K in thin-walled quartz tubes 4.0 mm in diameter. Second-order corrections were taken into account in calculations of the spin-Hamiltonian parameters for the V^{4+} ions.[18] Diphenylpicrylhydrazyl (g_0 = 2.0036) and Mn^{2+} ions in the MgO matrix were used for exact calibration of the magnetic field magnitude. The amount of paramagnetic sites in the sample was determined by double integrating of spectra and comparison with the standard single crystal of $CuCl_2 \cdot 2H_2O$ with the known number of spins. Experimental ESR spectra were processed using the computer program written and kindly presented by Prof. A. Kh. Vorob´ev (Department of Chemistry, M. V. Lomonosov MSU).

Results and Discussion

The ESR spectra for the samples of the V-2 series with different vanadium concentrations are presented in Fig. 1. At low concentrations ($[V^{4+}] \leq 0.3$ at.%), the spectrum appears as a well resolved multiplet typical of the paramagnetic V^{4+} ions, which substituted the Ti^{4+} ions in nodes of the crystalline rutile lattice[19,20] (tetragonal chain lattice, octahedral triangular coordination O/t, type $T^{K}_{O/t}$—SB $C4$, space group $D_{4h}{}^{14}$—$P4/mnm$).[21] In the rutile lattice, each [TiO_6] octahedron has two edges common with neighbors and forms chains.[21] The incorporation of the V atoms does not remarkably change the parameter of the rutile lattice to $[V^{4+}] \approx 4$ at.% ($a = b = 4.4923$ Å, $c = 2.8930$ Å). These parameters somewhat increase ($a = b = 4.5131 \pm 0.005$ Å, $c = 2.9073 \pm 0.003$ Å) at a greater content (4—5 at.%). During doping, beginning from $[V^{4+}] = 3$ at.%, a pair of lines appears in the diffraction patterns of both series (V-1 and V-2). These lines do not belong to TiO_2, and we could not identify them.

It is seen from the data in Table 1 that the spin-Hamiltonian parameters measured by independent authors differ noticeably. To determine the main values of

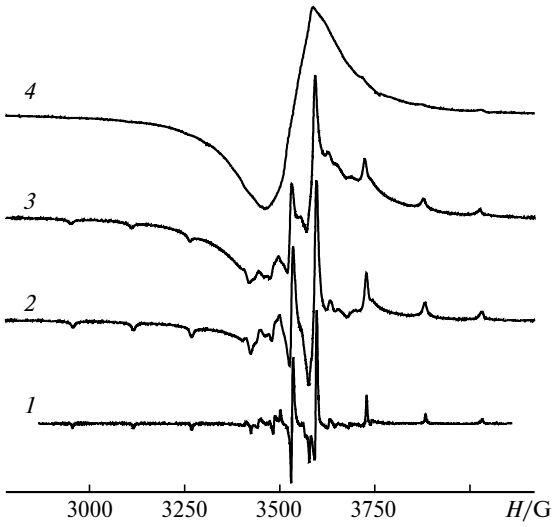

Fig. 1. ESR spectra of TiO_2 doped with V^{4+} ions at 77 K: $[V^{4+}]$ = 0.1 (*1*), 1 (*2*), 2 (*3*), and 5 at.% (*4*).

the $\hat{g}$- and $\hat{A}$ tensors, we simulated the experimental ESR spectra on a computer, which allowed the g_x, g_y and A_x, A_y parameters characterizing x—y anisotropy in the equatorial plane of the polyhedron to be calculated with good accuracy. Our results are closest to the published data[19,22,24] (see Table 1). In the samples of the V-1 series at $[V^{4+}] < 0.2$ at.%, lines corresponding to the interstitial V^{4+} ions, whose fraction is small and decreases rapidly with an increase in the content of the V^{4+} ions, are observed against the background of the main ESR spectrum (type *A*, see Table 1). The ESR parameters for this signal

Table 1. Parameters of ESR spectra (g_x, g_y, g_z, A_x, A_y, A_z) of rutile doped with the V^{4+} ions

Rutile sample	g_x	g_y	g_z	A_x	A_y	A_z	Refs.
				G			
V-1 (type *A*)	1.915	1.913	1.958	31.8	45.5	151.3	—*
V-1 (type *B*)	1.986	1.9935	1.9405	48.5	64.5	121.5	—*
V-2	1.9152	1.913	1.9583	31.87	45.5	151.25	—*
PC	1.913	1.913	1.956	31	45	156	19
PC	1.914	1.912	1.956	35	49	156	20
MC	1.915	1.913	1.956	34.7	48.1	155.5	22
MC	1.913	1.912	1.955	34.6	49.4	155	23
MC	1.9865	1.9930	1.9407	49	65	123	24
TiO_2**	1.917	1.893	1.966	39.1	45.3	153.6	25
NC	1.906	1.899	1.941	31	51	152	26

Note. PC is polycrystalline TiO_2, MC is monocrystalline TiO_2, and NC are nanocrystals of TiO_2. The accuracy of measurement of the parameters: $g_{x,y,z}$, ±0.004, $A_{x,y}$, ±2 G, and A_z, ±3 G.

* Data of this work.

** Calculated values.

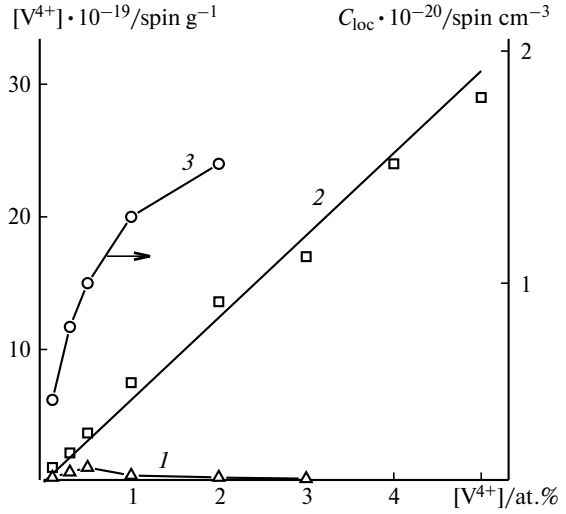

Fig. 2. Total content of the V^{4+} paramagnetic sites in doped polycrystalline TiO_2 without annealing (*1*) and with annealing at 900 °C in air (*2*) and the local concentration C_{loc} (*3*) of the isolated V^{4+} ions at different vanadium concentrations.

(type *B*, see Table 1) virtually coincide with the data obtained[24] for rutile single crystals.

An increase in the content of the V^{4+} ions first results in broadening (δH) of the individual components of the ESR spectrum (see Figs. 1 and 2) due to the magnetic dipole-dipole interaction,[27,28] and then a broad singlet line, whose fraction monotonically increases up to $[V^{4+}]$ = 5 at.% (see Figs. 1—3), appears against the background of the continuing increase in δH. Thus, at $[V^{4+}] \geq 1$ at.% the ESR spectra are the superposition of the multiplet spectrum, which characterizes isolated (magnetically diluted) V^{4+} ions, and the singlet with $g_0 = 1.935 \pm 0.005$ and linewidth $\Delta H \approx 14.0$ mT typical of the V^{4+} sites coupled by the strong spin-exchange interaction.[29] These sites are localized in microphases with a high local concentration $[V^{4+}]_s$/mol L^{-1}, which can be

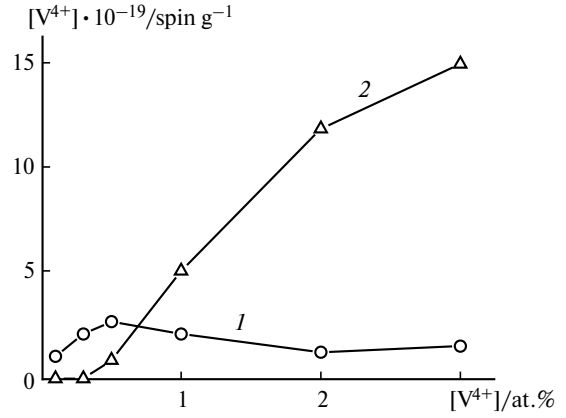

Fig. 3. Concentrations of the isolated (*1*) and associated (*2*) V^{4+} ions at different concentrations of the VO_2 microphase in the doped polycrystalline rutile.

estimated in the region of exchange narrowing (see Ref. 29) of the spectrum using the correlation

$$\nu_{solid} = K_{solid}[V^{4+}]_s^2 = 3.0 \cdot 10^{11} \cdot (\Delta H)^{-1}, \quad (1)$$

where ν_{solid} and K_{solid} are the frequency and rate constant, respectively, of statical spin exchange in the solid state ($K_{solid} = 1.8 \cdot 10^8$ s^{-1} (g-ion $L^{-1})^{-2}$ for the VO^{2+} vanadyl ions in solutions vitrified at 77 K), and ΔH/G is the linewidth.[29]

Substituting the experimental ΔH value, we obtain $[V^{4+}]_s \approx 3.5$ mol L^{-1}, from which it follows that the mean distance $\langle d \rangle_s$ between the paramagnetic V^{4+} ions in the regions of a high local concentration is ~7.7 Å according to the equation $\langle d \rangle_s = 10^8 \cdot ([V^{4+}]_s \cdot N_A)^{-1/3}$ (N_A is Avogadro´s number). The found $\langle d \rangle_s$ value more than twofold exceeds the distance between the adjacent metal ions in the lattices of TiO_2 and VO_2 single crystals ($d \approx 3.0$ Å),[21] indicating the formation of mixed titanium-vanadium oxide microphases $\{TiO_2—VO_2\}$ with a high V^{4+} content in the rutile samples at degrees of doping higher than 1 at.%.

Computer analysis of the ESR spectra provided an additional quantitative information on the PC rutile structure doped by the V^{4+} ions. Double integrating of the spectra showed (see Fig. 2) that in the samples of the V-2 series all vanadium ions are paramagnetic (within the experimental error) and distributed either as isolated V^{4+} ions in the TiO_2 matrix or in the $\{TiO_2—VO_2\}$ microphases. The fractions of the V^{4+} ions (β) in the indicated microphases, depending on the degree of doping, were determined by the subtraction of the singlet line from the ESR spectra of the samples of the V-2 series (see Fig. 3).

When the doped sample contains oxygen vacancies (V-1 series), the content of the V^{4+} paramagnetic sites is approximately constant but by several times lower than that in the V-2 samples at the same total dopant concentrations, *i.e.*, at $[V^{4+}] > 0.5$ at.% the main fraction of vanadium ions is in the diamagnetic state. Now we cannot unambiguously explain the above facts; so additional studies will be performed. Note that no broad singlet line in the ESR spectra of all V-1 samples was observed up to $[V^{n+}]$ = 5 at.%.

It is known[27,28] that the mean local concentration of paramagnetics (C_{lok}) in the zones of their localization can be determined by measuring the dipole-dipole broadening value δH of the lines of the ESR spectra in the solid matrix

$$C_{loc} = \delta H/A, \quad (2)$$

where $\delta H = \Delta H - \Delta H_0$ (ΔH is the width of the individual line in the ESR spectrum, and ΔH_0 is the width in the absence of dipole interaction); A is the coefficient depending on the space distribution of paramagnetic sites in the sample, the shape of the individual line, and time of

the spin-lattice relaxation (T_1) of the broadening paramagnetic.[28] For the VO^{2+} vanadyl and V^{4+} vanadium ions, $T_1 \geq 10^{-8}$ s, *i.e.*, spin-lattice relaxation exerts no effect on the width and shape of the ESR line.[27,28]

The C_{loc} values in the microphases with the isolated V^{4+} sites in the TiO_2 matrix were determined using Eq. (2) from the concentration broadening of the first and seventh components of parallel orientation of the spectrum (see Fig. 2). The value $A_{theor} = 5.8 \cdot 10^{-20}$ G cm^3 (see Ref. 28) was used in calculation under the assumption that the V^{4+} ions are arranged in the sites of the regular cubic sublattice (Gaussian line shape). It follows from Fig. 2 that at $[V^{4+}] > 0.5\%$ the mean distances $\langle r \rangle = C_{loc}^{-1/3}$ between the V^{4+} ions in the microphases of the slightly doped TiO_2 lattice become much longer than those calculated (r_{calc}) from $[V^{4+}]$ for doped rutile (for example, for the $Ti_{1.99}V_{0.01}O_2$ sample $\langle r \rangle$ = 2.0 nm at r_{calc} = 1.53 nm). This also indicates that some vanadium ions form the $\{TiO_2—VO_2\}$ microphases dissolved in TiO_2 already at the degree of doping of 1 at.%.

The results of studying the electroconductivity and photoelectrochemical properties of the samples confirm the ESR data. For example, the electroconductivity of the V-1 samples increases slowly to 2.0 Ohm^{-1} cm^{-1} with an increase in the V^{4+} concentration to 1 at.%. The further increase in the vanadium concentration results in a decrease in the electroconductivity of the samples to ~0.1 Ohm^{-1} cm^{-1}. Such a behavior can be explained by the formation of a mixed $\{TiO_2—VO_2\}$ microphase, whose exact composition is yet unclear. A similar behavior is demonstrated by the V-2 samples with a lower electroconductivity. We believe that in both series the character of spatial distribution of the doping vanadium ions in the rutile lattice is identical and caused by processes that occur during calcination (1200 °C). Therefore, the character of the microphases designated as $\{TiO_2—VO_2\}$ and their composition are similar in the V-1 and V-2 samples. However, in the case of the V-2 series, these mixed microphases contain the V^{4+} ions (due to additional oxidative annealing), and for the V-1 series, they contain the V^{3+} ions because annealing was not carried out.

The spectral curves of the photocurrent for the samples doped with the V^{4+} ions (Fig. 4) show that an increase in the vanadium concentration shifts the maximum of the main absorption toward short wavelengths, whereas its absolute value decreases (for convenience, all maxima in Fig. 4 were normalized to the same value) and the region of long-wave absorption is simultaneously extended to 800 nm.

For the samples synthesized at 1200 °C, the long-wave absorption threshold at low V^{4+} concentrations is 1.77 eV, and at $[V^{4+}] \geq 2$ at.% it becomes equal to 1.5 eV. These results suggest that doping the samples by vanadium results in different phases: the vanadium-doped rutile and a solid solution of VO_2 in TiO_2 with a relatively narrow

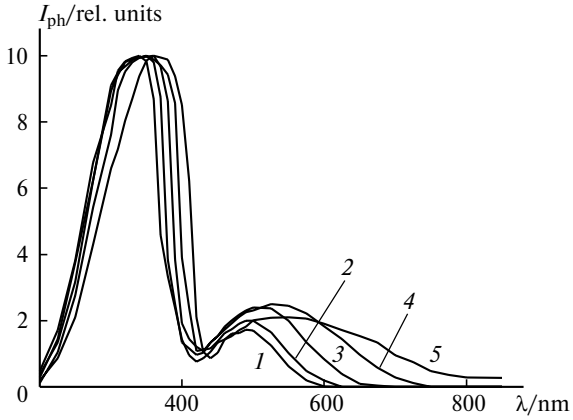

Fig. 4. Photocurrent (I_{ph}) spectra for the samples doped with 0.5 (*1*), 1 (*2*), 2 (*3*), 3 (*4*), and 5 at.% (*5*) of vanadium.

band gap. An increase in $[V^{4+}]$ increases the fraction of the $\{VO_2—TiO_2\}$ solid solution, which increases the long-wave photosensitivity and sharply decreases the electroconductivity of the samples. As a result, the photoelectrolysis current for these samples is lower than that for the non-doped samples despite a rather broad region of the long-wave photosensitivity in the spectral curves of the photocurrent. Since a sufficiently high voltage (up to 8—10 V) was applied to the sample in detection of the spectral curve, all generated carriers contribute to the photoresponse. The photoelectrolysis process was studied without application of a voltage from an external source and, hence, the carriers generated in the sample depth by the long-wave light recombined in the semiconductor bulk before their escape to the semiconductor surface and involvement in redox reactions. New microphases appeared at high $[V^{4+}]$ concentrations deteriorate the photoelectrochemical properties of the electrodes. This is seen in the plots of the integral photoelectrolysis current *vs.* vanadium concentration presented in Fig. 5.

Hence, we can conclude that a milder regime of thermal treatment is needed for the preparation of the effi-

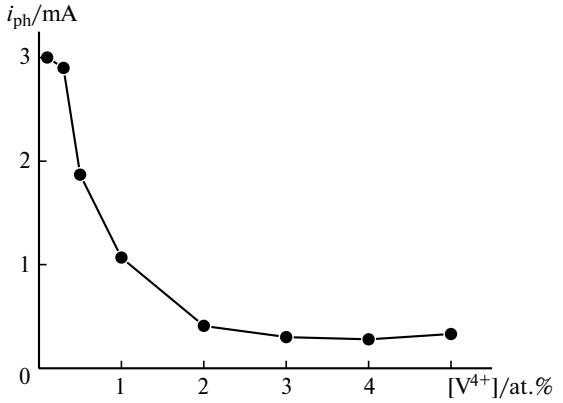

Fig. 5. Plot of the integral photocurrent (i_{ph}) *vs.* vanadium percentage.

cient photoelectrodes based on the vanadium-doped TiO_2 sensitive in the long-wave spectral region. To obtain the samples containing no microphases of the $\{TiO_2—VO_2\}$ type, one should perform the synthesis, most likely, at lower temperatures (≤1100 °C) and for longer time.

The authors thank V. I. Pergushov (M. V. Lomonosov MSU) and A. A. Pridantsev (ICP, RAS) for help in experiments and useful discussions and A. A. Shubin (IC, SB of the RAS) for help in calculation of the ESR spectra.

This work was financially supported by the Russian Foundation for Basic Research (Project Nos. 00-03-81168 and 99-03-33252a).

References

1. I. E. Wachs, R. Y. Saleh, S. S. Chan, and C. Chersich, *Appl. Catal.*, 1985, **15**, 339.
2. G. Centi, E. Giamello, D. Pinelli, and F. Trifiro, *J. Catal.*, 1991, **130**, 220.
3. *Fotokataliticheskoe preobrazovanie solnechnoi energii* [*Photocatalytic Conversion of Solar Energy*], Ed. K. I. Zamaraev, Nauka, Novosibirsk, 1985, **1**—**2**, 520 pp. (in Russian).
4. *Photocatalysis: Fundamentals and Applications*, Eds. N. Serpone and E. Pelizzetti, J. Wiley and Sons, New York, 1989.
5. M. R. Hoffmann, S. T. Martin, W. Choi, and D. W. Bahnemann, *Chem. Rev.*, 1995, **95**, 69.
6. *Photocatalytic Purification and Treatment of Water and Air*, Eds. D. F. Ollis and H. Al-Ekabi, Elsevier, Amsterdam, 1993.
7. *Energy Resources through Photochemistry and Catalysis*, Ed. M. Grätzel, Academic Press, New York, 1983, 472 pp.
8. *Photoelectrochemistry, Photocatalysis and Photoreactors*, Ed. M. Schiavello, Reidel Publ. Co., Dordrecht, 1985.
9. *Photochemical Conversion and Storage of Solar Energy*, Eds. E. Pelizzetti and M. Schiavello, Kluwer, Dordrecht, 1991.
10. Yu. V. Pleskov, *Fotoelektrokhimicheskoe preobrazovanie solnechnoi energii* [*Photoelectrochemical Conversion of Solar Energy*], Nauka, Moscow, 1990 (in Russian).
11. A. K. Ghosh and H. P. Maruska, *J. Electrochem. Soc.*, 1977, **124**, 1516.
12. T. E. Phillips, K. Moorjani, J. C. Murphy, and T. O. Poehler, *J. Electrochem. Soc.*, 1982, **129**, 1210.
13. P. Salvador, *Solar Energy Materials*, 1980, **2**, 413.
14. Y. Matsumoto, J. Kurimoto, T. Shimizu, and E. Sato, *J. Electrochem. Soc.*, 1981, **128**, 1040.
15. A. G. Sarkisyan, V. M. Arakelyan, G. M. Stepanyan, R. S. Akopyan, E. L. Ignatyan, and A. L. Margaryan, *Uch. Zap. Erevan. Gos. Un-ta* [*Scientific Writings of Yerevan State University*], 1981, No. 1, 79 (in Russian).
16. V. M. Arutyunian, in *Hydrogen Energy Progress*, **XII**, Eds. J. C. Bolcich and T. N. Veziroglu, EAAH, Buenos Aires, 1998, **1**, 13.
17. A. G. Sarkisyan, V. M. Arutyunian, G. M. Stepanyan, A. A. Pogosyan, and E. A. Khachaturyan, *Elektrokhim.*, 1985, **21**, 261 [*Sov. Electrochem.*, 1985, **21** (Engl. Transl.)].
18. H. A. Kuska and M. T. Rogers, *ESR of First Row Transition Metal Complex Ions*, Interscience Publ., New York, 1968.
19. A. Davidson and M. Che, *J. Phys. Chem.*, 1992, **96**, 9909.
20. R. Gallay, J. J. van der Klink, and J. Moser, *Phys. Rev.*, 1986, **34B**, 3060.
21. B. F. Ormont, *Struktura neorganicheskikh veshchestv* [*Structure of Inorganic Substances*], Gostekhteorizdat, Moscow, 1950, 968 pp. (in Russian).
22. H. J. Gerritsen and H. R. Lewis, *Phys. Rev.*, 1960, **119**, 1010.
23. G. M. Zverev and A. M. Prokhorov, *Zh. Eksperim. Teor. Fiz.*, 1960, **39**, 222 [*J. Exp. Theor. Phys.*, 1960, **39** (Engl. Transl.)].
24. F. Kubec and Z. Sroubek, *J. Chem. Phys.*, 1972, **57**, 1660.
25. F. M. Michel-Calendini and G. Fichelle, *Phys. Stat. Sol. B.*, 1975, **69**, 607.
26. S. T. Martin, C. L. Morrison, and M. R. Hoffmann, *J. Phys. Chem.*, 1994, **98**, 13695.
27. A. Abragam, *The Principles of Nuclear Magnetism*, Clarendon Press, Oxford, 1961, 480 pp.
28. Ya. S. Lebedev and V. I. Muromtsev, *EPR i relaksatsiya stabilizirovannykh radikalov* [*ESR and Relaxation of Stabilized Radicals*], Khimiya, Moscow, 1971, 256 pp. (in Russian).
29. Yu. N. Molin, K. M. Salikhov, and K. I. Zamaraev, *Spin Exchange*, Springer-Verlag, Berlin, 1980, 242 pp.

Received July 18, 2001;
in revised form June 4, 2002